Nuclear Waste Form/Package Performance, Behavior and Lifetime

T. Ahn

U.S. Nuclear Regulatory Commission, USA

ABSTRACT

Examples of analytical approaches and methodologies for modeling the behavior of waste forms and waste package metals in long-term management of spent nuclear fuel (SNF) and high-level waste (HLW) are presented. Two cases − i) long-term geological disposal, and ii) interim extended dry storage − are considered. The waste package (or canister) that serves as a barrier is dependent upon the performance of construction metals. Corrosion degradation modes of the construction metals are evaluated. The waste behavior during SNF degradation is also evaluated. In each mode of corrosion or degradation, the associated risk insights are discussed with respect to public safety in the system performance of disposal or storage.

Disclaimer:

The NRC staff views expressed herein are preliminary and do not constitute a final judgment or determination of the matters addressed or of the acceptability of any licensing action that may be under consideration at the NRC.

1. Introduction

This chapter presents example analytic approaches and methodologies for modeling the behavior of waste forms and different metals used in packaging spent nuclear fuel (SNF) and high-level waste (HLW). The long-term behavior of waste forms and different metals used packaging SNF and HLW are important attributes in assessing safety and security associated with nuclear waste management. This behavior is a core component in determining radionuclide source-term and/or criticality control, used in assessing radionuclide release to the human environment. The assessments and modeling of the long-term behavior of the waste form and different metals are further complicated by a variety of environmental conditions, including natural and man-induced external hazards. This is especially true when the purported waste management time is very long, e.g., several thousand years or beyond.

The approaches and methodologies presented in this chapter also cover model uncertainties that affect assessment of the public health and safety.

The content of this work is considered by the U.S. Nuclear Regulatory Commission (NRC) which assesses cases for management of SNF and HLW in the U.S. The NRC is preparing risk and performance insights. Information that NRC obtained from the past activities in the management of SNF and HLW in U.S., along with relevant information from different international programs is included.

In the U.S., the long-term management of SNF and HLW is considered for *geological disposal* for thousands of years and beyond, and interim *extended dry storage* of SNF for up to 300 years. In both management cases, materials performance issues related to waste form and corrosion of different construction metals are considered, i.e., container metal in waste packages used for geological disposal, and canister construction metal for the extended dry storage. The following four topics related to the waste-form dissolution and corrosion are addressed in this paper: (i) long-term integrity of passive film, slow general corrosion, and localized corrosion of different metals; (ii) stress corrosion cracking (SCC) of carbon steel and stainless steel; (iii) SNF degradation; and (iv) cladding performance. The discussion of each topic addresses how it applies to the two management cases, as appropriate. Broader performance issues of waste form and different metals under the two management cases are also discussed. Finally, risk insights are addressed with respect to performance (or risk) assessment for the disposal or storage system. Both management cases incorporate laboratory data, analytical models, archaeological (for disposal) and/or industrial (for extended dry storage and disposal). Some similar classes of metals are used in both cases for different purposes. For example, stainless steels are primarily used for extended storage, but may also be considered for disposal. On the other hand, carbon steel is mainly applied in disposal.

2. Background

For each topic in the performance evaluation of waste form and waste package (or canister), the associated risk in the disposal or extended storage system needs to be considered. Three risk related questions are addressed: (i) what can go wrong, (ii) how likely is it, and (iii) what are the consequences? Various time-dependent or one-time behaviors of waste form and waste package are assessed with respect to these three questions. To answer the first question, features, events and processes (FEP) for the geological disposal options (Nuclear Energy Agency, 1997), or equivalent (e.g., NRC, 2007; Dasgupta, 2002) are identified. Regarding the second question, the identified FEPs or their equivalents are evaluated with respect to given system designs considering normal conditions and accident conditions from man-made and natural hazards. Once the likelihood or probability of a FEP, or its equivalent, exceeds a threshold value, its consequence is assessed in terms of confinement failure, radionuclide release, nuclear subcriticality and radiation shielding, or other performance objectives of the total system or subsystems, and thus, addressing the third question. The implementations of these three questions are iterative in nature with the modifications of design details, until risk assessment or design performance objectives are met. This iterative process also allows early identification of risk-significant issues related to different designs.

Based on the iterative process, the following FEPs associated with the behavior of waste package or storage canister construction metals are considered significant in the two management cases.

- Long-term integrity of protective passive film for corrosion-resistant metals such as nickel-based alloys, titanium alloys or stainless steel: This allows low general corrosion rates for these metals, keeping the waste package or storage canister intact for a long time.

- Low oxygen or sulfur ion concentration in the reducing aqueous environment for corrosion-allowance metals such as copper or carbon steel: This also allows low general corrosion rates for these metals, keeping the waste package or storage canister intact for a long time.
- Low susceptibility to localized corrosion: Low ratios of chloride to nitrate ion concentrations prevent localized corrosion in nickel-based alloys and stainless steel. Low fluoride ion concentration prevents fast titanium dissolution without loss of adherent protective passive metal-oxide film. Carbon steel is susceptible to pitting in the reducing environment is minimal.
- Low susceptibility to SCC and/or hydrogen-induced cracking: The magnitude of residual stress or concentrations of chemical species such as carbonate ions in solution or salt deposits determine a metal or alloys susceptibility to SCC and/or hydrogen-induced cracking.
- Low initial manufacturing defects: Allows minimum early mechanical failure of waste package and canister due to manufacturing defects, for all metals considered.

Similarly, the following FEPs related to the waste form are potentially important for containing the SNF or HLW in the two management cases.

Conditions affecting dissolution, solubility of actinides: Environmental conditions such as reducing aqueous groundwaters results in very low dissolution rates of fission products and low solubility of actinides in SNF dissolution. This limits the radionuclide release in the biosphere. Similarly, near neutral pH of the aqueous environment also results in low dissolution rates of fission products and solubility limits for actinides in HLW glass dissolution (BSC, 2004).

- Conditions affecting performance of cladding: Conditions such as low hydrogen absorption, temperature, and residual stress in cladding minimize hydrogen-induced cladding failure.

- The high burnup SNF encased by the cladding may increase or decrease the radionuclide release fraction, affecting radionuclide release in air.

In the following sections 3 to 6, selected specific subtopics from the above list are discussed in depth.

3. Long-Term Integrity of Passive Film, Slow General Corrosion, and Localized Corrosion of Disposal Container

This section presents the general corrosion behavior of passive and non-passive metal and alloys in mild and near-neutral pH environments such as tuff or granite hostrock sets. Both tuff and granite will have reducing groundwater, whereas tuff can also have oxidizing groundwater. In a long period of geological time (e.g., several thousand years), a container of a finite thickness is expected to fail even at very slow general corrosion rates. Under more aggressive aqueous environmental conditions that may evolve during the disposal, localized corrosion (e.g., crevice corrosion or pitting corrosion) may occur, decreasing the container life time in a very short time (e.g., months to years). The first case to be discussed is long-term integrity of a protective passive film in nickel-based alloy, resulting in very low general corrosion rates. The

second case is corrosion-allowance, carbon steel in reducing aqueous environments resulting in very low general corrosion rates. These two cases are discussed further regarding susceptibility to localized corrosion. Finally, risk insights of the general corrosion and localized corrosion in a disposal system are discussed with respect to this type of container with low general corrosion rate or possible susceptibility to localized corrosion.

3.1. Long-term integrity of passive film of nickel-based alloy

In the absence of severe localized corrosion conditions, nickel-based alloys containing chromium are protected against fast corrosion by a chromium-rich oxide adherent film commonly known as "passive film" at the exposed surface. Typical examples are the thin, adherent passive oxide films observed on sample surfaces after short-term polarization tests and long-term immersion tests (Orme, 2005; NWTRB, 2002). Filmthicknesses were in the range of a few nanometers (10^{-9} meters, nm, 3.9 x 10^{-10} inch) and tended to be rich in chromium (III) oxides (Cr_2O_3 and/or $NiCr_2O_4$). A thick outer layer was also observed on top of the inner chromium-rich oxide layer. The outer layer was typically porous and consisted mostly of nickel oxide and the oxides of some other alloying elements. The chromium-rich oxide is considered to protect the bare metal against rapid corrosion in the long-term, i.e. geological time frames. A cross-sectional view of passive film formed on the surface of annealed nickel-based alloy is presented in Figure 1 (Orme, 2005). It is important to understand whether the passive layer persists for a long period of time or not (Ahn, et al., 2008a). A number of issues have been studied to determine whether the protective layer remains stable in the long-term. For example, if the protective layer grows continuously, the stress may build up at the interface of the bare metal and the protective layer, and the protective layer may spall off. However, the subsequently exposed bare metal would repassivate. Certain metalloids such as sulfur may be segregated at the interface during the anodic dissolution of bare metal surface. A potential mechanism of the breakdown of the passive film induced by enrichment of sulfur at the metal-passive film interface is presented in Figure 2 (Marcus, 1995). When the surface concentration of the segregated sulfur exceeds a critical value, the protective layer will become unstable. The bare metal exposed as a result the unstable protective layer may repassivate after dissolution of the accumulated sulfur layer. Other impurity elements such as silicon in the alloys or solutions may also affect the long-term stability of the protective layer. Microbially-influenced corrosion may also destabilize the protective layer. However, the bare metal surface formed after the destabilization of the protective layer could repassivate.

An important related issue is the accuracy in measuring very low general corrosion rates. General corrosion rates on the order of nm/year are difficult to measure accurately. The accuracy is important because the rates must be extrapolated to a very long time period to calculate the extent of general corrosion and assess when the package would fail.

Once the passive film becomes unstable without repassivation during the disposal, either high general corrosion would occur or localized corrosion such as crevice corrosion or pitting corrosion would occur. For localized corrosion to be initiated, if there is no existing (propagating) pitting or crevice corrosion, the corrosion potential needs to reach the breakdown potential for highly corrosion resistant alloys (such as nickel-based alloys) (Ahn, et al., 2008b; ASM International,1987). This condition is determined by the severity of the evolved groundwater chemistry. More conservatively, at the corrosion

potential below the repassivation potential, even the existing (propagating) pitting or crevice corrosion will be arrested. The breakdown potential or repassivation potential generally increases with higher concentration ratios of oxyanions such as nitrates to chloride (Dunn, et al., 2005). Even if the localized corrosion occurs, it is not expected to open up entire areas of a container surface. The cathodic capacity of the outside of an active crevice or pit, from the separated cathodic area from the active area, will limit localized corrosion propagation fronts (Shukla, et al., 2007). Some studies show only pit growth rather than uniform dissolution in the crevice area of highly corrosion-resistant alloys (Ahn, et al., 2008a). Based on the cathodic capacity limitation, a maximum of 20 % of the surface area is likely to be open (He, et al., 2011).

3.2. Carbon steel corrosion in mild reducing aqueous environments

Carbon steel is a corrosion-allowance metal that is expected to have relatively low corrosion rate in a mild, near-neutral pH, and reducing environment such as granite and clay(Jung, et al., 2011). One localized corrosion process in carbon steel is pitting corrosion. This pitting process is empirically represented by a "pitting factor," which is defined as a ratio of pit penetration depth to the uniform corrosion depth. Therefore, degradation by pitting corrosion of a carbon steel container can be represented by adjusting the magnitude of the general corrosion rates.

Even in an underground repository which is planned in the long-term to have a reducing environment, it will initially have an oxidizing condition due to the excavation conducted before closure (which provides oxygen). The general corrosion rate of carbon steel in an oxidizing environment is very high: in the range of 10 to 100 μm/year (3.94×10^{-4} to 3.94×10^{-3} inch/year) at room temperature in simulated mild initial groundwater (Jung, et al., 2011). During 30 year oxidizing conditions applicable for carbon steel corrosion, a general corrosion rate of 50 μm/year (1.97×10^{-3} inch/year) will result in a small penetration depth of 0.15 cm (0.02 inch). Estimating the carbon-steel general corrosion rate using laboratory data and analogue data indicates corrosion rates in the range of 0.1 to 10 μm/year (3.94×10^{-6} to 3.94×10^{-4} inch/year) in the reducing environment (Yoshikawa, et al., 2008; David, et al., 2002). Figure 3 shows the data collected from Yoshikawa, et al., (2008) from Japan and David, et al., (2002) from France.

.

Carbon steel is susceptible to pitting corrosion in an oxidizing environment. In addition, carbon steel is expected to corrode at higher general rate in an oxidizing compared to a reducing environment. However, the effect of pitting corrosion can be accounted for by using an enhanced general corrosion rate. The pitting factor, which is a ratio of pit propagation depth to general corrosion penetration depth, will approach unity during the oxidizing period as the general corrosion proceeds deeper. The pitting does not enhance the corrosion penetration at this point. An example case is shown in Figure 4 (Johnson and King, 2000).

3.3. Risk insights of general corrosion and localized corrosion

Container failure by general corrosion is likely to result in sufficient opening of the container surface to allow substantial advective release of radionuclides. The rate of release of radionuclides by advective release is expected to be higher by several orders of magnitude than diffusive release that may occur through tight cracks or small pits. Therefore, underestimating the general corrosion rates because of the uncertainties may

lead to an inaccurate, delayed and low-magnitude radionuclide release from a failed container. When the uncertainties associated with the general corrosion rates are random in nature, the general corrosion rates are expressed in a uniform distribution, either in a linear scale or in a log scale, depending on characteristics of the uncertainties. Figure 5 is an example output of the failure probability of a carbon steel container with time, using the range of general corrosion rates sampled from a log normal distribution extracted from Figure 3 (David, et al., 2002) (Jung, et al., 2011). The radionuclide release at a given time will begin from a finite number of containers that failed, from calculations using the probability of failure and the total number of containers.

Container failure by localized corrosion may also limit the radionuclide release because of restricted flow through the small perforations due to the of pits. Pit diameters were from micrometers to millimeters (0.4 microinch to milliinch) and pit density is 0.1 – 100/cm^2 (0.6 – 645/inch^2) as shown in Figure 6 from selected metals and aqueous environments (Szklarsks-Smialowska,1986). In addition, the pits are usually filled with corrosion products or solid precipitates from groundwater. Therefore, radionuclide release through the restricted area is likely to be diffusive, which is generally slower than advective release.

4. Stress Corrosion and Hydrogen-Induced Cracking of Carbon Steel and Stainless Steel

This section presents the SCC behavior of carbon steel disposal containers and stainless steel storage canisters. Carbon steel is mostly susceptible to hydrogen-induced cracking due to residual weld stress or seismic-induced impact stress. Hydrogen is generated during general corrosion or gamma radiolysis of groundwater in a reducing environment (Ahn and Soo, 1995).

In a marine (coastal) environment, salt deposits may occur on the stainless steel canister surface due to salt water droplets in the air. The salt deposits on the canister when the canister surface temperature is above ambient. Aqueous conditions of high chloride concentration will form due to this salt deliquescence. With the residual tensile stress at welds, this high concentration of chlorides may induce SCC (Shirai, et al, 2011; EPRI, 2005). SCC can be screened out based on stress mitigation techniques such as applying compressive stress in the weld. In the absence of this mitigation, the opening surface area by SCC (or hydrogen-induced) cracks can be estimated. This quantitative estimate allows assessment of the radionuclide release due to waste form degradation inside the container or the canister.

4.1. Hydrogen-induced cracking of carbon steel

Carbon steel may be susceptible to hydrogen-induced cracking (Kobayasi, et al., 2011). Hydrogen is likely to be produced by radiolysis of groundwater and by water reduction during the corrosion process in reducing conditions. Figure 7 shows reduction in area versus applied potential in constant extension rate testing (CERT) for ASTM A216-Grade WCA steel in concentrated synthetic groundwater at 80 ºC (Ahn and Soo, 1995). This hydrogen-induced cracking can be regarded as a variation of SCC. Recently, the surface opening area resulting from SCC container damage has been assessed for various candidate container metals including carbon steel. Generally, maximum opening

area is approximately 0. 1 % of the total surface area of the waste package (Gwo, et al., 2011). This original assessment was made with impact stress in the deformed area of the container as an effect of seismic impact. However, this assessment can be applicable to the normal static case too. The weld residual stress and a weld area can be used instead of impact stress and deformed area from seismicity. The models for estimating opening area due to SCC are described in the following section for stainless steel canisters. This approach is equally applicable to the hydrogen-induced cracking of carbon steel.

4.2. SCC of stainless steel

Salt deposits on the canister surface open to the environment are likely to be significant in coastal areas. SCC of the stainless steel canister needs to be considered when the relative humidity (RH) in air is appropriately high and the amount of salt deposits is sufficient to form aggressive and sufficient aqueous conditions at welds to initiate SCC. If the RH is too low, the aqueous condition will not exist. On the other hand, if RH is too high, the chloride concentration will not be high enough to initiate SCC. The weld area could have residual tensile stress and sensitized microstructure which is prone to SCC.

The RH of the environment surrounding the canister surface and salt deposits depend on the canister surface temperature. Over a long time, the surface temperature will decrease as the radioactivity inside the canister gradually decays. This will result in increasing RH of the environment immediately adjacent the canister surface. Also, temperature, RH and the amount of salt deposits will not be homogeneous on the canister surface because the SNF storage configuration and air flow surrounding the canister. In addition, the weld areas will be primarily susceptible to SCC. Considering these environmental and materials factors, the probability associated with SCC could be low enough for it to be screened out from Performance assessment (PA).

When SCC occurs, radionuclide releases may be primarily caused by the release of aerosol radioactive materials, which may in turn be driven by the pressure of inert fill gas and fission gas inside the canister (from prior release from failed cladding). The release rates are also affected by the opening area of the canister surface caused by SCC. The SCC area density per weld area of the canister can be estimated conservatively by the following equation (Gwo, et al., 2011):

$\delta = C\,\sigma/E$	(1)

where

δ	—	crack areal density (m^2/m^2)
σ	—	applied stress (MPa)
E	—	Young's modulus (MPa)
C	—	geometric constant

For example, a calculation for stainless steel using Eq. (1) suggests that the crack areal density per unit weld area is approximately 1.2×10^{-3} at 170-310 MPa (25 – 45 ksi) of applied stress, (193-207) x 10^3 MPa [(28 – 30) x 10^3 ksi] of Young's modulus (Gwo, et al., 2011). The weld area fraction is about 10^{-2} – 10^{-1} of total surface area (ASM International, 1990). In a canister surface area of about 30 m^2 (4.6 x 10^4 $inch^2$), the

surface opening area will become 3.6 x (10^2 – 10^3) mm^2 (0.56 – 5.6 $inch^2$). The model in Eq. (1) is conservative, assuming a distribution of uniform crack size. In reality, the number and size of cracks are likely to be smaller. On the other hand, larger cracks may form, depending on the incipient crack size. In any case, this calculated area is obviously larger than that allowed for leak tightness (Institute for Nuclear Materials Management, 1997).

4.3. Risk insights of the cracking of carbon steel and stainless steel

Figure 8 shows an example of the radionuclide release fraction to the environment from a cask (Sprung, et al., 2000). Casks include canister and other overpacks. Strictly speaking, this figure was constructed for a transportation cask. Nevertheless, the radionuclide release behavior would be similar in the storage cask. The radionuclide release fraction is expressed by (1.0 – Retention). In this range of the surface opening area, the surface opening is already wide enough to result in the release fraction approaching to 1. This retention mechanism is in addition to the low radionuclide release fraction from the degraded UO_2 matrix and the failed cladding. In reality, the surface area opening by SCC may be smaller because the model of Eq. (1) is conservative.

Figure 9 [calculated using "beta Scoping of Options and Analyzing Risk (SOAR) model" (Markley, et al., 2011)] shows an example of a calculation of radionuclide release from the seismic-induced SCC of various disposal containers (Gwo, et al., 2011). There is an additional factor lowering the magnitude of radionuclide release due to the restricted perforation made by SCC.

5. SNF Degradation

This section presents the degradation behavior of SNF in mild and near neutral environments under (i) oxidizing or reducing aqueous disposal conditions and (ii) in dry storage environments. During the aqueous dissolution of SNF highly soluble fission products such as Tc-99 or I-129 are released congruently with (i.e., in proportion to) the SNF matrix (UO_2) dissolution. On the other hand, actinides such Pu-239 or Np-237 are released at a concentration below or equal to their solubility limits (or colloid concentration), which are in turn determined by the SNF matrix dissolution rate, groundwater flow rate and solubility limit. Colloids are suspended solid particles of less than 1 micrometer in size that can contain actinides. An oxidizing aqueous environment promotes electrochemical dissolution of the SNF matrix in soluble species with the aid of oxidants such as dissolved oxygen and hydrogen peroxide (Shoesmith, 2000). In a reducing environment, the UO_2 matrix will dissolve chemically in soluble species (Sunder and Shoesmith, 1991). Generally, the electrochemical dissolution rate is faster than the chemical dissolution rate. In the presence of radiolysis effects, the SNF matrix may dissolve in either electrochemical or chemical process, depending on the magnitude of the radiolysis (Ahn, et al., 2011a). In conjunction with container failure and sorption and/or flow behavior of backfill, the SNF matrix dissolution serves as the source term of radionuclide release in the PA. In a dry storage environment, mechanical degradation of the SNF matrix could occur by air oxidation/humid air hydration or impact fragmentation upon the canister failure under normal conditions (e.g., SCC failure) or external hazard conditions (e.g., aircraft or seismic impact). In the canister, if incomplete drying of SNF assemblies occurs, the residual water may increase RH sufficiently to oxidize (by oxygen

from the radiolysis of water molecules) or hydrate the SNF matrix. With severe external hazards, high temperatures or impact stress may fragment the SNF matrix by oxidation or mechanical disintegration. The respirable SNF particles (i.e., suspended aerosol, less than 10 μm [3.9 microinch] in size) produced by the fragmentation serve as the primary source term for radionuclide release in air.

5.1 SNF dissolution

The dissolution rates by the electrochemical and chemical processes are (Ahn,1996a):

$R_{dis} = \frac{S}{V} k_e f(E)$	(2)
and $R_{dis} = \frac{S}{V} k_-(C_S - C_t)$	(3)
$R_{dis} = \frac{A}{V} k_+(C_t - C_0) + \frac{F}{V} C_t + N_{par} C_t$	(4)

where

S	—	surface area of the dissolving phase
V	—	leachate volume
k_e	—	rate constant for electrochemical dissolution
$f(E)$	—	dissolution rate as a function of electrochemical potential E
k_-	—	rate constant for SF dissolution
C_s	—	effective solubility limit of dissolving phase
C_t	—	elemental concentration under consideration
k_+	—	rate constant for growth of the reprecipitated phase
F	—	flow rate of ground water
N_{par}	—	formation or growth rate of colloids per unit leachate concentration

Eq. (2) is for electrochemical process, Eq. (3) is for chemical process, and Eq. (4) is for release rate from the dissolution processes of the first two equations.

The fractional mobilization rate is the dissolution rate multiplied by the specific surface area of the SNF matrix. Conservatively, the fractional mobilization rates can be assumed constant within uncertainty ranges at a given temperature. The environmental conditions are important in determining the dissolution rates, including near field water chemistry, temperature, pH, or reducing or oxidizing conditions. Important water chemistry includes carbonates, and cations such as calcium or silica species (Ahn and Mohanty, 2008c).

In connecting the dissolution rate to the fractional mobilization rate, the specific surface area is determined by the average fragment size (radius) and density of the waste form. Typically, the fragment size of commercial SNF is 0.1 cm [0.04 inch] (Ahn and Mohanty, 2008c)

If the temperature exceeds 100 °C [212 ºF], solid-state oxidation or hydration will occur, depending on the RH. Higher uranium oxides ($UO_{2.4}$ or U_3O_8) that form by oxidization of the UO_2 matirx dissolve at a rate similar to the unoxidized UO_2 matrix. Hydrated $UO_3 \cdot xH_2O$ (x = 0.8, 2) dissolves 10-20 times faster than unhydrated oxides. However, the rate of hydration (i.e., the formation rate of $UO_3 \cdot xH_2O$) is slower than the aqueous dissolution rate. Ahn and Mohanty (2008c) summarized the effects of oxidation and hydration on the dissolution.

5.2 Colloid formation and solubility limit

Actinides such Pu-239 or Np-237 have low solubility limits, and they are released at a concentration below or equal to their solubility limits (or colloid concentrations), which in turn are determined by the SNF matrix dissolution rate, groundwater flow rate and solubility limit.

Regarding colloid formation, Ahn (1996a) summarized the processes involved. During the dissolution of the SNF matrix, suspended solid particles containing mainly actinides of low solubility may form. The colloids can carry a large amount of actinides compared with dissolved species. The traditional processes of colloid formation (especially in actinide colloids) have been investigated under near-equilibrium conditions. Most studies in this regard pertain to chemical bonding among ions. Extending the chemical bonding process in equilibrium or non-equilibrium states, colloid formation may be described in macroscopic ways by three different processes: (a) condensation, (b) dispersion, and (c) sorption (pseudo-colloid formation). Colloids may form by precipitation in small particles because of supersaturation of actinides or the SNF matrix (i.e., condensation). The layer of the precipitated phases on the SNF matrix can be mechanically detached into small suspended particles (i.e., dispersion). Finally, the dissolved pure actinide species can be sorbed on the surface of nonradioactive inert groundwater colloids (i.e., sorption). Figure 10 shows schematics of these three processes (CRWMS M&O, 2001).

5.3 Dry oxidation or hydration, and mechanical fracture

Dry-air oxidation or humid air hydration of SNF in air or in the presence of limited amounts of groundwater may play an important role in radionuclide releases (Ahn and Mohanty, 2008c; Ahn, 1996b). The UO_2 matrix will fracture (or crack) upon oxidation or hydration by volume change. Lower oxidized oxides such as $UO_{2.4}$ will contract, whereas higher oxides such as U_3O_8 or UO_3 hydrates will expand. Lower and higher oxides are defined here as oxides with a (O/U) ratio smaller and larger than 2.4, respectively. Fractions (e.g., 10^{-6} - 10^{-3}) of oxidized or hydrated phases are likely to be respirable aerosol less than 10 micrometer (3.9 microinch) in size. The aerosol will increase the radionuclide release in air. The oxidized or hydrolyzed phases also increase the area of SNF surface exposed to groundwater. This increase of the exposed surface area is in turn expected to increase radionuclide release in groundwater. Similarly, mechanical impacts such as those caused by seismic events can also fragment the SNF into particles. Figure 11 shows the fraction of respirable particles, depending on the impact energy absorbed. The fine-grained and porous rim structure near cladding of high burnup (above about 60 GWd/MTU) UO_2 may also affect the magnitude of the radionuclide release fraction (NRC, 2007).

5.4 Risk insight of SNF degradation

Table 1 summarizes of the dissolution rates for oxidizing and reducing disposal environments (Ahn, et al., 2011a) used in a performance assessment model SOAR model" (Markley, et al., 2011). A range of environmental conditions are considered, mostly near-neutral pH and ambient temperature. The variation of pH and temperature can be adjusted in terms of dissolution rate as user-defined parameters. For this base case, radionuclide release is estimated combining the reducing and oxidizing environments, to simulated residual radiolysis of water by actinides in the reducing environment. Figure 9 shows the estimated dose from the radionuclide release for this combined case.

Considering all radionuclide release fractions from the storage canister, and from the UO_2 matrix, an exercise was conducted to estimate the doses to workers or members of the public from air borne fragments of the SNF matrix caused by SNF oxidation and SNF drop/collision (after Kamas, et al., 2006). The most significant dose contributor in the release fraction is aerosol SNF fines (i.e., small solid particles). Tritium, noble gases, iodine, crud, ruthenium, cesium, strontium and SNF fines were part of the source term considered. In Figure 12, the radionuclide release fraction of the aerosol SNF fines, 2.0×10^{-6} for drop/collision case and 1.2×10^{-3} for SNF oxidation case were used to estimate the dose to workers or members of the public (Ahn et al., 2011b; Kamas, et al., 2006). A site boundary was defined, for the dose to workers within the boundary and to members of the public outside the boundary.

The left figure is for SNF oxidation under normal operations. The Wake effects are a modification of radionuclide transport path right outside the cask storage building due to building shadow. Consequently, radionuclide transport will stop. Within a short distance from the building, the radionuclide transport will not be reached. The right figure is for drop/collision cases. In both cases, arbitrary dose rate units are used for the log scale. The oxidation case gives a dose rate ten times higher than the collision case in the same log-scale unit.

6. Cladding Performance

This section presents the performance of cladding in (i) aqueous disposal environments and (ii) dry storage environments. Hydrogen-induced cracking of cladding is a major detrimental degradation mechanism for both disposal and storage conditions. Crack opening area allows radionuclide release under both conditions. Oxidation (or general corrosion) of cladding is very slow and localized corrosion is unlikely to occur in near neutral-pH disposal environments (Ahn, 1996b). Oxidation of cladding is only possible in the presence of residual water and/or oxygen in dry storage canisters. Initially-defective cladding may be further cracked (unzipped) by the pressure imposed on it by corrosion products of the SNF matrix or zirconium itself. Longer longitudinal cracks that develop from the initial cracking/unzipping will increase radionuclide release under both conditions.

6.1. Hydrogen effects

During reactor operations, the cladding metals, mainly Zircaloy, corrode in water. This introduces hydrogen into the Zircaloy. Hydrogen can degrade the strength of Zircaloy through overall embrittlement caused by a dispersion of radially-oriented hydrides (perpendicular to thehoop stress) (Chung, 2004). The hydrides formed during reactor

operations are mostly circumferential hydrides (parallel to the hoop stress). Circumferential hydrides may not affect the strength significantly, depending on the magnitude of severity. However, circumferential hydrides are known to become radially-reoriented in the presence of appropriate applied stress and temperature (Chung, 2004). Figure 13 compares hydrides oriented circumferential or perpendicular to the hoop stress and Figure 14 shows ductility loss with radial hydrides (Yagnik, et al., 2004). Another hydrogen effect is delayed-hydride cracking (DHC). Small cracks that develop on the inner or outer surface of cladding may lead to crack propagation when assisted by hydrogen diffusion to the crack tip, thus forming radially-oriented hydrides at the crack tip. The mechanism has not been proven to exist under the dry storage conditions, although data are available under reactor operational conditions (Ahn and Rondinella, 2011). Figure 15 shows a schematic for the mechanism of the DHC process. If it happens under dry storage conditions, it will be more likely for higher burnup SNF (e.g., above 60 GWd/MTU). The crack density and size from hydrogen embrttlement of hydride reorientation and DHC can be conservatively assessed like the SCC of stainless steel described in Section 4.2.

6.2. Unzipping of cladding

A maximum of 1 % of SNF discharged from reactors could be defective. Volume expansion associated with the oxidation/hydration of the SNF matrix or zirconium may crack/unzip defective cladding (Cunnane, et al., 2003). Figure 16 shows a schematic of this unzipping process (DOE, 2002). Unzipping was observed in the Argonne National Laboratory 1.5-year long tests, caused by stress generated by corrosion-product accumulation in the gap of cladding and the fuel matrix from uniform corrosion of Zircaloy cladding at 175 $^{\circ}$C [347 $^{\circ}$F] (Cunnane, et al., 2003).

Oxidation/hydration may occur with either residual moisture inside the intact canister or container, or from moisture that has intruded into the failed canister or container. This cladding failure may affect the magnitude of the radionuclide release fraction and challenge the retrievability of the SNF materials, and lead to configuration changes in internal structure that impact nuclear criticality.

6.3. Risk insight of cladding performance

The values of crack opening from models need to be compared with those used in determining the radionuclide release fraction in storage from experimental work (Lorentz, et. al., 1980). Lorentz, et al. (1980) conducted burst tests by heating a clad SNF rod, allowing an opening area of about 1.6 cm^2 (~10^{-1} fraction of the total cladding surface). If the calculated value of the cladding area opened by cracking resulting from hydrogen effects is smaller than that from the experiments by Lorenz, et al. (1980), the radionuclide release fraction will not increase with further cladding cracking from the embrittlement. Otherwise, the radionuclide release fraction from the UO_2 matrix to the canister inside will be affected by the embrittlement. The current regulation for SNF storage (Part 72) requires that the cladding must be protected during storage against degradation that leads to gross rupture or the SNF needs to be otherwise confined. Gross rupture of cladding may challenge the UO_2 retrievability and threaten the maintenance of nuclear subcriticality.

The effects of crack opening on the radionuclide release in disposal were also studied. Ahn and Mohanty (2008c) summarized the literature results. In the presence of partial protection from failed cladding by cracking, the dissolution rate decreases significantly

compared to bare SNF, with slit (~0.015 cm [5.9 x 10. inch] width and ~ 2.54 cm [1 inch] length) or hole (- 0.02 cm [7.9 x 10^{-3} inch] diameter) defective SNF cladding under immersion conditions in J-13 well water at 85 °C [185 °F]. The tests were intended to simulate cladding partially failed by localized corrosion or SCC. The radionuclide release rates decreased by a factor of ~140 for Tc-99, ~7 x10^{5} for I-129, and ~ 65 for Sr-90, compared to bare CSNF. However, in the segment tests of clad SNF under immersion conditions, the radionuclide release rates did not decrease compared to bare SNF. In these tests, nearly half of the surface area was exposed. Similar conclusions can be drawn from tests with Canadian Deuterium-Natural Uranium Reactor CSNF, immersed in Canadian granitic groundwater. These results suggest that cladding would not inhibit the dissolution rates if it fails catastrophically exposing a substantial surface area to the solution (groundwater).

Elam et al. (2003) assessed the effects on nuclear subcriticality caused by the configuration changes due to cladding failure. The main assumption in this study is full water flooding in the cask. The report presented the reactivity for various SNF rod conditions. For uniform burnup of 45 and 75 GWd/MTU collapsed SNF rods, the variations of the neutron multiplication factor, Δk_{eff}, were not significant for this changed cladding configuration.

7. Summary

This chapter presented examples of analytic approaches and methodologies for modeling the behaviors of waste forms and waste package metals in long-term management of spent nuclear fuel (SNF) and high-level waste (HLW). Two cases − i) long-term geologic disposal, and ii) interim extended dry storage –were considered.

Selected important topics in the management were presented on:

(i) long-term integrity of passive film, slow general corrosion, and localized corrosion in disposal container: the role of passive film was discussed in terms of long-term slow general corrosion, and fast localized corrosion upon the passivity breakdown in corrosion-resistance metals, and slow general corrosion of corrosion-allowance metals in the reducing environment.
(ii) SCC of carbon steel and stainless steel was discussed with respect to their performance in disposal or storage.
(iii) spent nuclear fuel degradation process was discussed in terms of radionuclide release in disposal and storage systems.
(iv) cladding performance was discussed in terms of radionuclide release and criticality control in disposal and storage systems.

In each topic, the involved risk insights were also discussed in the system safety assessment in disposal and storage.

8. References

All NRC ADAMS documents can be found at <www.nrc.gov/reading-rm/adams.html> using the accession number (MLxxxxxx).

Ahn, T., “Long-term Kinetic Effects and Colloid Formation in the Dissolution of LWR Spent-fuel,” NUREG-1564, U.S. Nuclear Regulatory Commission, Washington, D.C., 1996a. NRC ADAMS ML073100056.

Ahn, T., “Dry Oxidation and Fracture of LWR Spent-fuels,” NUREG-1565, U.S. Nuclear Regulatory Commission, Washington, D.C., 1996b. NRC ADAMS ML040150720.

Ahn, T., H. Jung, E. L. Tipton, and T. Sippel, “Model Abstraction of Waste Form Degradation in Alternative Disposal Site,” Proceedings of 2011 International Radioactive Waste Management Conference (IHLRWMC), Albuquerque, New Mexico, April 10-14, Paper No. 3396, 2011a.

Ahn, T., H. Jung, X. He, and O. Pensado. “Understanding Long-Term Corrosion of Alloy 22 Container in the Potential Yucca Mountain Repository for High-Level Nuclear Waste Disposal.” *Journal of Nuclear Materials.* Vol. 379. pp. 33-41, 2008a.

Ahn, T., X. He, H. Jung and P. Shukla, “Long-Term Electrochemical Criteria for Crevice Corrosion in Potential Repository Environments at Yucca Mountain, Nevada,” ASTM Seminar, Accelerated Testing of Materials in Spent Nuclear Fuel and High Level Waste Storage System, ASTM International Subcommittee C26.13 Spent Fuel and High Level Waste, Tampa, FL, January 27 – 31, 2008b. NRC ADAMS ML080080360.
Ahn, T., H. Jung, P. Shukla, and X. He, “Long-Term Electrochemical Criteria for Crevice Corrosion in Concentrated Chloride Solutions,” NRC ADAMS ML112010085, 2011

Ahn, T. and S. Mohanty, “Dissolution Kinetics of Commercial Spent Nuclear Fuels in the Potential Yucca Mountain Repository Environment,” NUREG-1924, NRC ADAMS ML 083120074, 2008c.

Ahn, T. and V. Rondinella, “Effects of Radiation-Induced Swelling of Spent Nuclear Fuel Matrix,” International Atomic Energy Agency (IAEA), Research Coordination Meeting (RCM)-1 of Coordinated Research Project (CRP)-III “Evaluation of Conditions for Hydrogen-Induced Degradation of Zirconium Alloys during Fuel Operation and Storage,” October 24 – 28, IAEA, Vienna, Austria, NRC ADAMS ML112900212, 2011.

Ahn, T. and P. Soo, “Corrosion of Low-Carbon Cast Steel in Concentrated Synthetic Groundwater at 80 to 150 °C,” *Waste Management,* 15, pp. 471-476, 1995.

Ahn, T, R. Sun, T. Wilt, S. Kamas and S. Whaley, “Source Term Analysis in Handling Canister-Based Spent Nuclear Fuel: preliminary Dose Estimate, NRC ADAMS ML112640440, 2011b.

ASM International, ASM Handbook, Formally Ninth Edition, Metals Handbook, Volume 13. Corrosion, 1987.

Bechtel SAIC Company (BSC), Defense HLW Glass Degradation Model, ANL-EBS-MD-000016 REV 02 ACN 01 ERD 1, Las Vegas, Nevada: Bechtel SAIC Company, 2004.

Chung, H. “Understanding Hydride- and Hydrogen-Related Processes in High-Burnup Cladding in Spent-Fuel-Storage and Accident Situations, Proceedings of 2004 International Meeting on LWR Fuel Performance, Orlando, Florida, September 19-22, 2004, Paper No. 1064.

CRWMS M&O, “Colloid-Associated Radionuclide Concentration Limits,” ANL-EBS-MD-000020 REV 00 ICN 01, Las Vegas, Nevada: Civilian Radioactive Waste Management System Management and Operating Contractor, 2001.

Cunnane, J., W. Ebert, M. Goldberg, R. Finch, and C. Mertz, “Yucca Mountain Project Report, Waste Form Testing Work,” Argonne National Laboratory, Chemical Technology Division, 2003.

Dasgupta, B., R. Benke, B. Sagar, R. Janetzke, and A. Chowdhury, “PCSA Tool Development, Progress Report II,” Version 2, San Antonio, TX: Center for Nuclear Waste Regulatory Analyses, 2002.

David, D., C. Lemaitre and C. Crusset, “Archaeological Analogue Studies for the Prediction of Long-Term Corrosion on Buried Metals,” pp. 242, EFC Series Vol. 36, Prediction of Long-Term Corrosion Behavior in Nuclear Waste Systems, Eds. D. Feron and D. D. Macdonald, European Federation of Corrosion Publications, Maney, London, 2002.

U. S. Department of Energy (DOE), Office of Civilian Radioactive Waste Management, Yucca Mountain Science and Engineering Report, Rev. 1, 2002

Dunn, D. S., O. Pensado, Y.-M. Pan, R. T. Pabalan, L. Yang, X. He and K. T. Chiang, “Passive and Localized Corrosion of Alloy 22 – Modeling and Experiments,” CNWRA 2005-02, Revision 1, Center for Nuclear Waste Regulatory Analyses, 2005.

Elam. K. R., J. C. Wagner and C. V. Parks, “Effects of Fuel Failure on Criticality Safety and Radiation Dose for Spent Fuel Casks, NUREG/CR-6835, U.S. Nuclear Regulatory Commission, 2003.

Electric Power Research Institute (EPRI), “Effects of Marine Environments on Stress Corrosion Cracking of Austenitic Stainless Steels,” EPRI 1011820, Palo Alto: California, EPRI, 2005.

Gwo, J., T. Ahn, and X. He, “Modeling Disruptive Events Using the β-SOAR Model: Levels of β-SOAR Model Flexibility in Applications and Initial Insights,” Proceedings of 2011 International Radioactive Waste Management Conference (IHLRWMC), Albuquerque, New Mexico, April 10-14, pp. 867-874, 2011.

He, X., O. Pensado, T. Ahn, and P. Shukla, “Model Abstraction of Stainless Steel Waste Package Degradation,” Proceedings of 2011 International Radioactive Waste Management Conference (IHLRWMC), Albuquerque, New Mexico, April 10-14, Paper No. 3460, 2011.

Institute for Nuclear Materials Management, “American National Standard for Leakage 12782 Tests on Packages for Shipment of Radioactive Materials,” ANSI N14.5, 1997.

Johnson, L. and F. King, “The Effect of the Evolution of Environmental Conditions on the Corrosion Evolutionary Path in a Repository for Spent Fuel and High-Level Waste in Opalinus Clay,” *Journal of Nuclear Materials,* 379, pp. 9-15, 2008*;* from JNC, H12: Project to Establish the Scientific and Technical Basis for HLW Disposal in Japan, Japan Nuclear Cycle Development Institute, Supporting Report 2, Repository Design and Engineering Technology, 2000.

Jung, H., T. Ahn, and X. He, “Representation of Copper and Carbon Steel Waste Package Degradation in a Generic Performance Assessment Model,” Proceedings of 2011 International Radioactive Waste Management Conference (IHLRWMC), Albuquerque, New Mexico, April 10-14, Paper No. 3353, 2011.

Kamas, S., T. Ahn and M. Bailey, “Pre-closure Safety Analysis: Sensitivity Studies and Preliminary Dose Results,” Proceedings of the 11th International High-Level Radioactive Waste Management Conference (IHLRWM), April 30 - May 4, Las Vegas, NV, pp.1096-1100, American Nuclear Society, LaGrange Park, Illinois, 2006.

Kobayashi, M., Y. Yokoyama, R. Takahashi, H. Asano, N. Taniguchi and M. Naito, “Long Term Integrity of Overpack Closure Weld for HLW Geological Disposal Part 2 – Corrosion Properties under Anaerobic Conditions,” The Fourth International Workshop on Long Term Prediction of Corrosion Damage in Nuclear Waste Systems, the Belgian Nuclear Research Centre (SCKNCEN) and the Belgian Agency for Radioactive Waste and Enriched Fissile Materials (ONDRAF/NIRAS), 2010, special issue of *Corrosion Engineering, Science and Technology*, 2011.

Lorenz, R. A., et al., “Fission product Release from Highly Irradiated LWR Fuel,” NUREG/CR-0722, Oak Ridge National Laboratory, pp. 48-80, 1980.

Marcus, P. “Sulfur-Assisted Corrosion Mechanisms and the Role of Alloyed Elements,” Chapter 8, pp. 239 - 263, in Corrosion Mechanisms in Theory and Practice, by P. Marcus and J. Oudar, Marcel Dekker, Inc., 1995.

Markley, C., E. L. Tipton, J. Winterle, O. Pensado, and J.-P. Gwo, “β-SOAR: A Flexible Tool for Analyzing Disposal of Nuclear Waste,” Proceedings of 2011 International Radioactive Waste Management Conference (IHLRWMC), Albuquerque, New Mexico, April 10-14, Paper No. 3455, 2011.

Nuclear Energy Agency. “An International Database of Features, Events, and Processes [Draft].” Nuclear Energy Agency Working Group on the “Development of a Database of Features, Events, and Processes Relevant to the Assessment of Post-Closure Safety of Radioactive Waste Repositories, Safety Assessment of Radioactive Waste Repositories Series.” United Kingdom: Safety Assessment Management Limited. June 24, 1997.

NRC, “A Pilot Probabilistic Risk Assessment Of a Dry Cask Storage System At a Nuclear Power Plant.” NUREG-1864, Washington, DC: NRC. 2007.

U.S. Nuclear Waste Technical Review Board (NWTRB), “Peer Review of the Waste Package Material Performance,” Waste Package Materials Performance Peer Review Panel, Final Report, February 28, 2002

Orme, C.A. "The Passive Film on Alloy 22." UCRL–TR–215277. Livermore, California: Lawrence Livermore National Laboratory. 2005.

Shukla, P., R. Pabalan, T. Ahn, L. Yang, X. He and H. Jung, “Cathodic Capacity of Alloy 22 in the Potential Yucca Mountain Repository Environment,” NRC ADAMS ML072780515, 2007.

Shirai, K., J. Tani, T. Arai, M. Wataru, H. Takeda, and T. Saegusa, “SCC Evaluation of Multi-Purpose Canister,” Proceedings of 2011 International Radioactive Waste

Management Conference (IHLRWMC), Albuquerque, New Mexico, April 10-14, Paper No. 3333, 2011.

Sprung, J. L., et al., "Reexamination of Spent Fuel Shipment Estimates," NUREG/CR-6672, Vol. 1, SAND2000-0234, Albuquerque, NM: Sandia National Laboratory; Washington DC: NRC. 2000.

Shoesmith, D. W., "Fuel Corrosion Processes under Waste Disposal Conditions." *Journal of Nuclear Materials,* 282**,** 1(2000).

Sunder, S. and D. W. Shoesmith, "Chemistry of UO_2 Fuel Dissolution in Relation to the Disposal of Used Nuclear Fuel," AECL-10395, Pinawa, Canada: Atomic Energy of Canada Limited (1991).

Szklarska-Smialowska, Z., in Pitting Corrosion of Metals, National Association of Corrosion Engineers, Houston, TX, p. 143 – 253, 1986.

Yagnik, S. K., R-C Kuo, Y. R. Rashid, A. J. Machiels, and R. L. Yang, "Effect of Hydrides on the Mechanical Properties of Zircaloy 4," Proceedings of the 2004 International Meeting on LWR Fuel Performance, Orlando, Florida, September 19-22, 2004, Paper 1089.

Yoshikawa, H., E. Gunji, and M. Tokuda, "Long Term Stability of Iron for More than 1500 Years Indicated by Archaeological Samples from the Yamato 6th Tumulus," *Journal of Nuclear Materials*, 379, 112, 2008.

Figure 1. A cross-sectional view of passive film form on the surface of annealed nickel-based alloy (Alloy 22, Ni-22Cr-13Mo-4Fe-3W) (Orme, 2005)

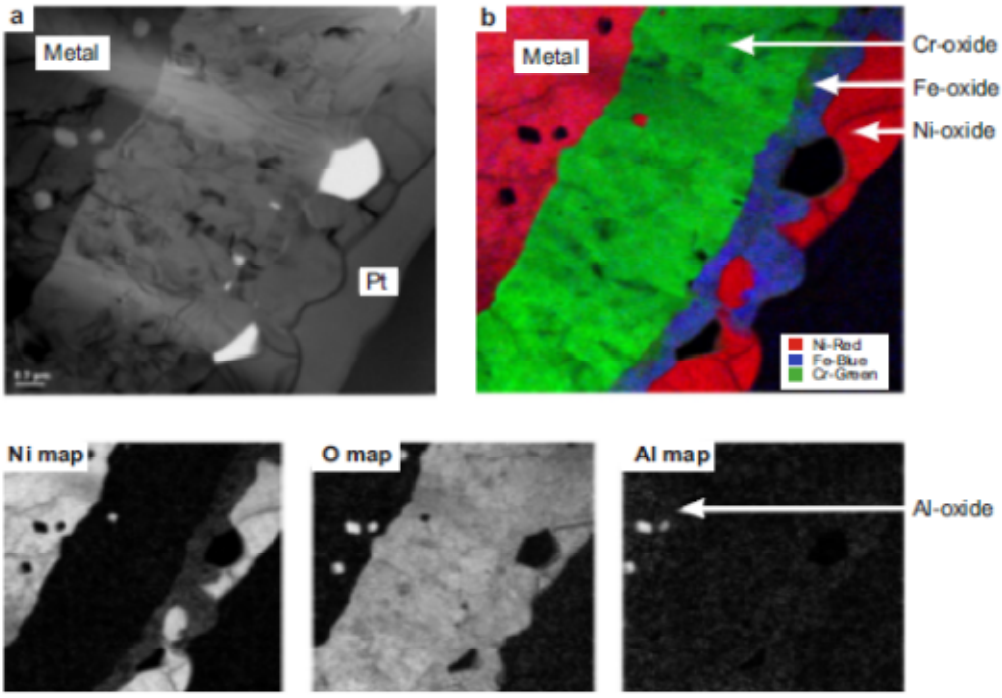

Figure 2. Mechanism of the breakdown of the passive film induced by enrichment of sulfur at the metal-passive film interface (Marcus, 1995) [copy right permission by Taylor and Francis for Marcel Dekker]

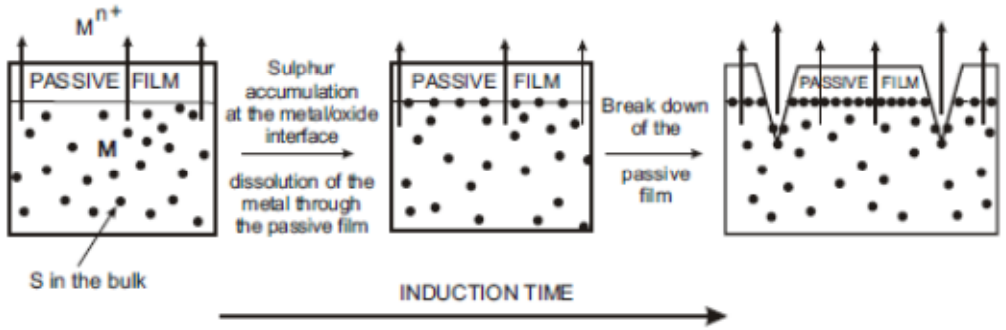

Figure 3. Measured corrosion rates of carbon steel in simulated solutions and correlation with archaeological analogue data up to 1,000 years: the first analysis was conducted in Japan, and the second in France

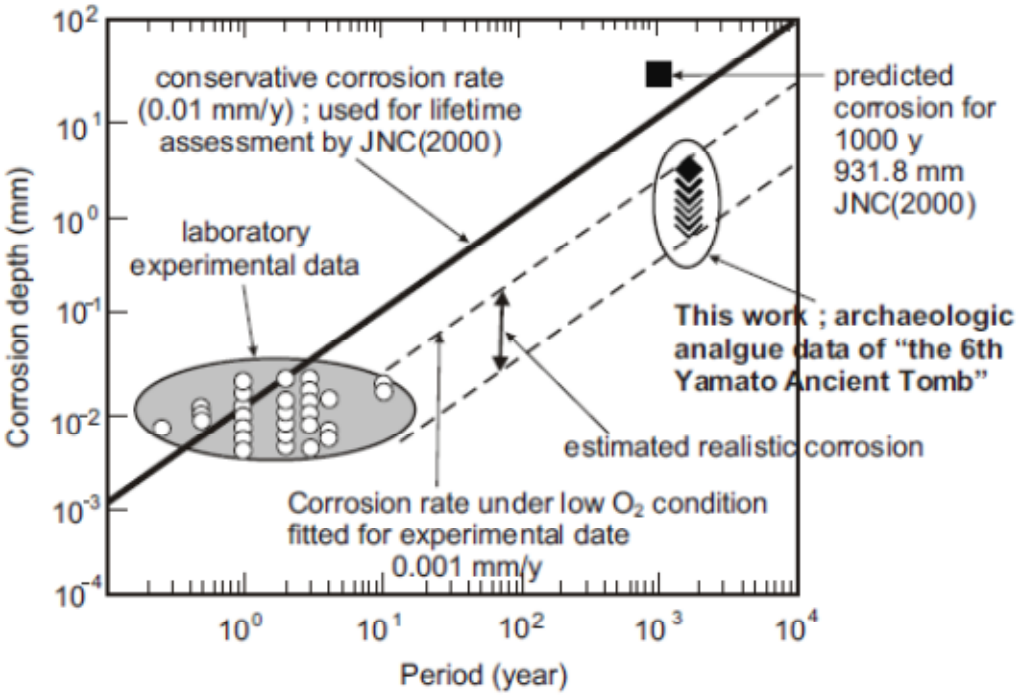

(Yoshikawa, et al., 2008) [copy right permission by Elsevier]

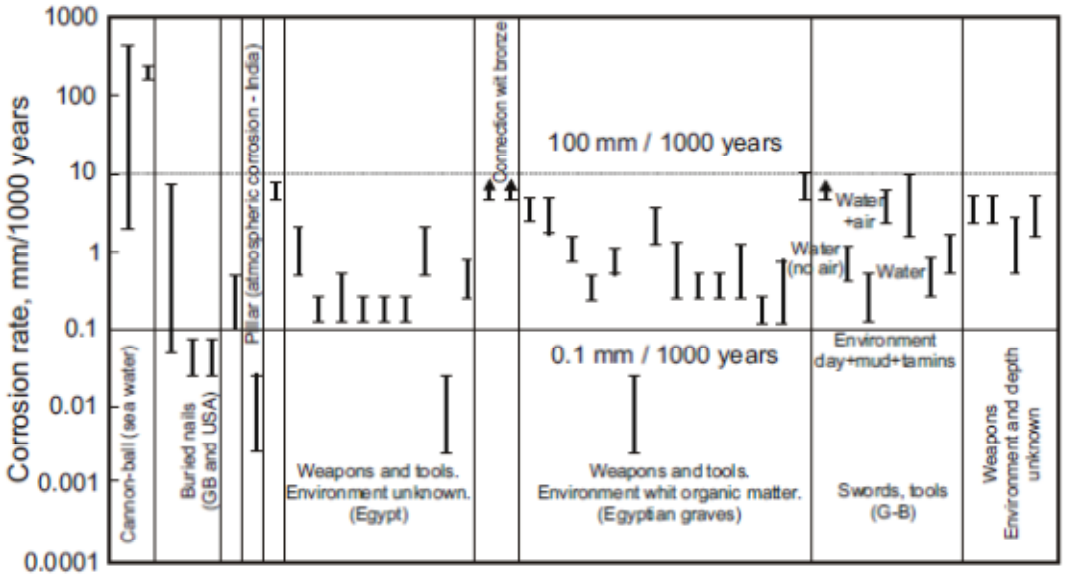

(David, et al., 2002) [copy right permission by Maney Publishing]

Figure 4. Variation of the pitting factor for carbon steel with the average depth of corrosion derived from long-term corrosion tests and short-term laboratory measurements (Johnson and King, 2008) [copy right permission by Elsevier]

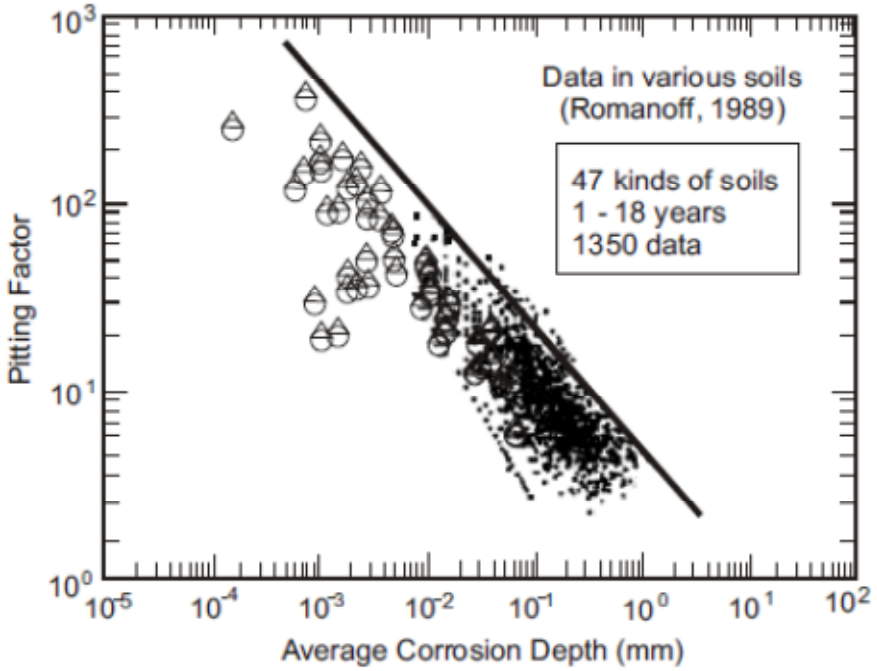

Figure 5. Carbon steel waste package failure time for geologic disposal system in reducing environment (Jung, et al., 2011) [copy right permission by ANS]

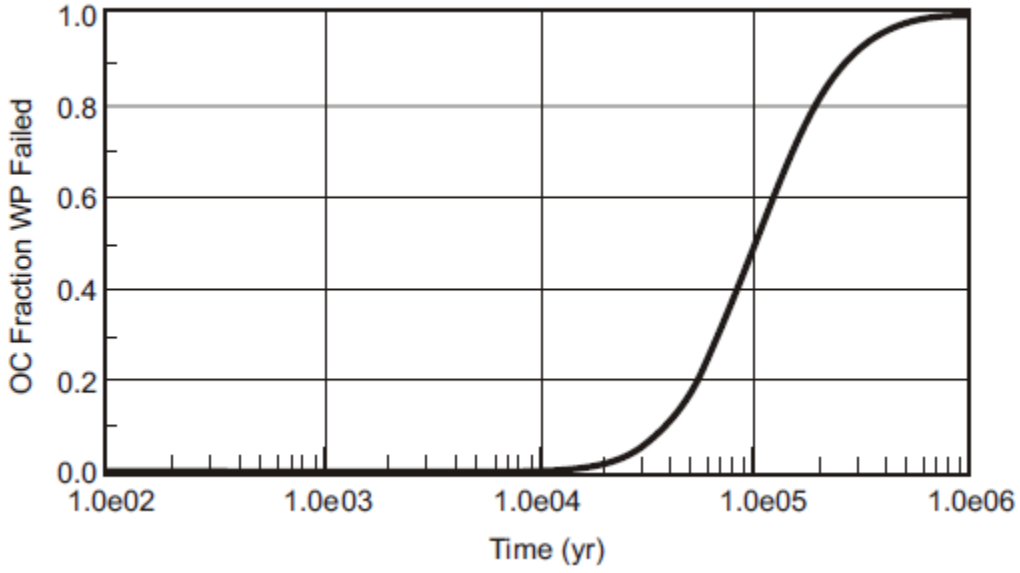

Figure 6. Examples of size and distribution of pits. Pit diameter vs time for 18Cr-12Ni-2Mo-Ti stainless steel in 0.1 N H_2SO_4 + 0.1 N NaCl. Normal pit size observed is in the range of micrometers to millimeters and pit density is for 304 stainless steel after potentiostatic polarization in 1 M NaCl solution. The term “d” is pit diameter and “t” is time (reprinted with permission) (Szklarsks-Smialowska, 1986) [copy right permission by

NACE]

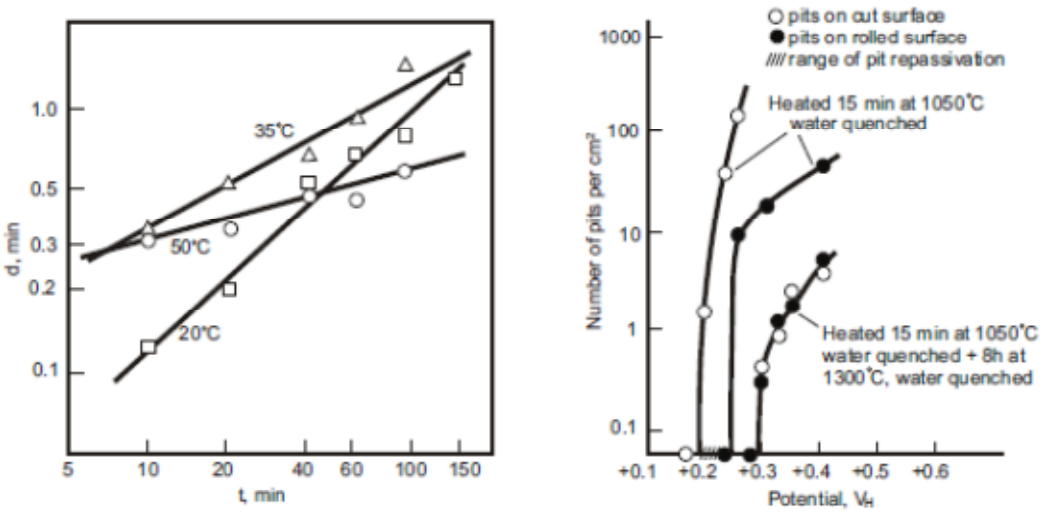

Figure 7. Reduction in area versus applied potential in constant extension rate testing (CERT) for ASTM A216-Grade WCA steel in concentrated synthetic groundwater at 80 ºC (Ahn and Soo, 1995) [permission by Elsevier]. The quantitative assessment of the opening surface area will be dealt in the presentation on stress corrosion cracking (opening surface area).

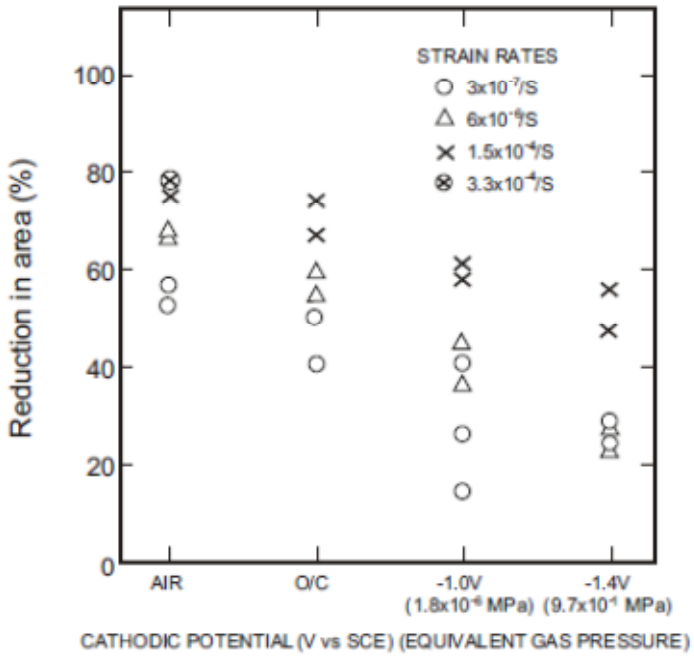

Figure 8. Cask-to-Environment Release Fractions (1.0 – Retention) Versus Open Cask Surface Area (Sprung, et al., 2000)

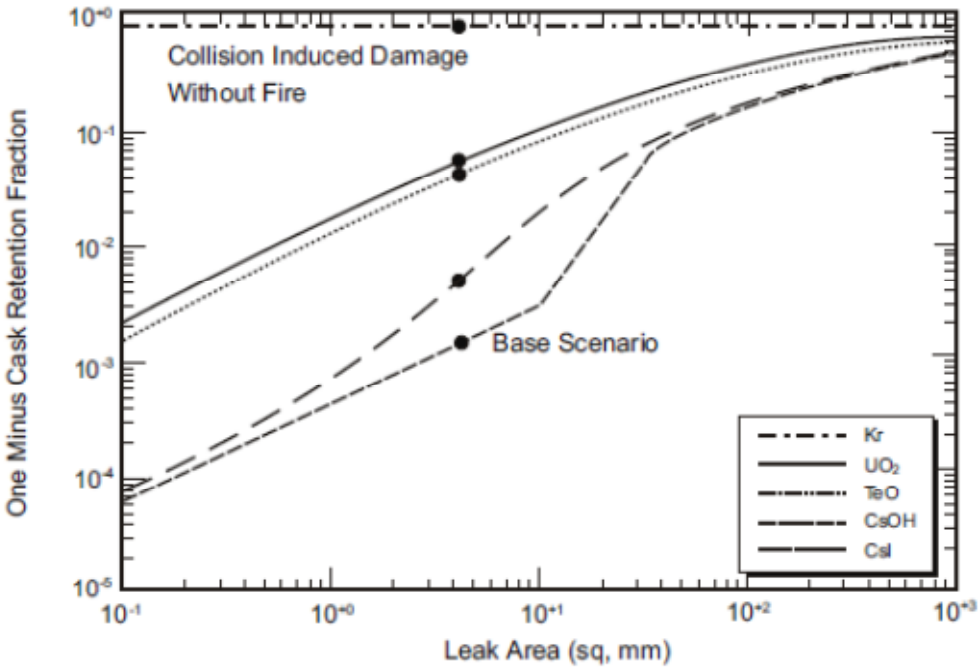

Figure 9. Example beta-SOAR (Markley et al., 2011) Dose Results for Only Commercial SNF Using Combined Degradation Rate in a Stylized Reducing Geologic Disposal System (Ahn, et al., 2011) [copy right permission by ANS]

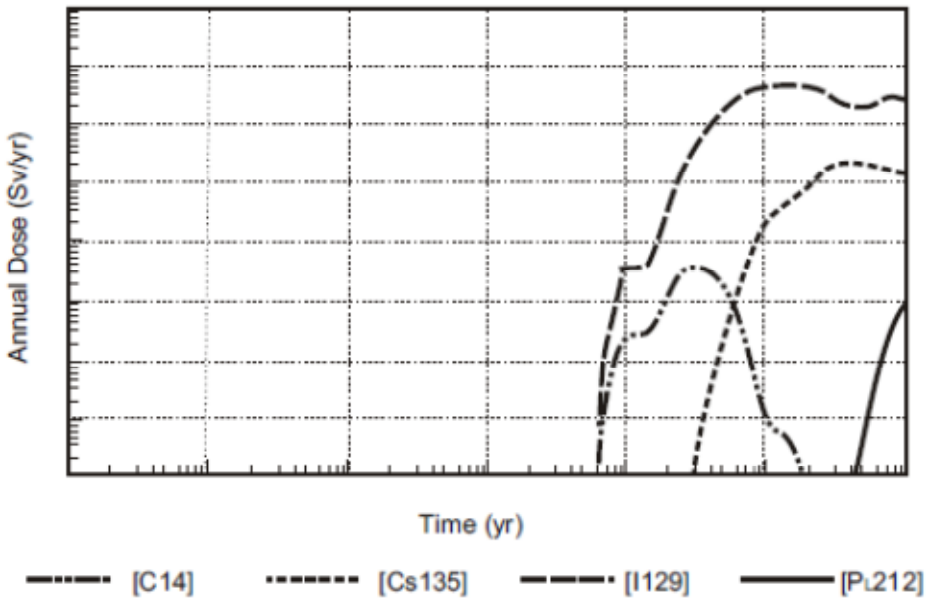

Figure 10. Types of colloid formation (CRWMS M&O, 2001)

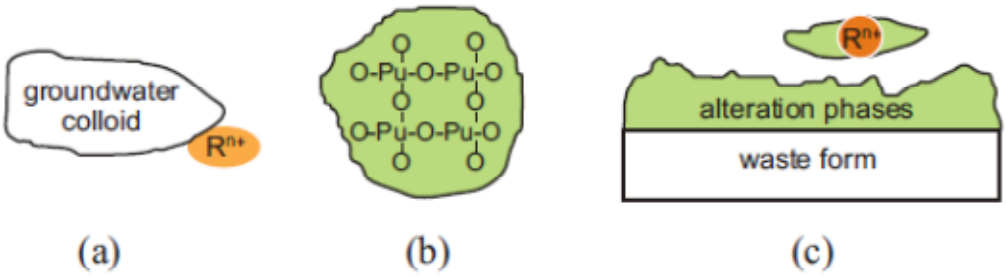

Figure 11. Comparison of the DOE handbook Respirable Fraction Equation to Experimental Values of the Specific Energy Input into the Brittle Material.(NRC, 2007). Specifc energy is the external impact energy (Joule) absorbed in a unit weight (g) of SNF.

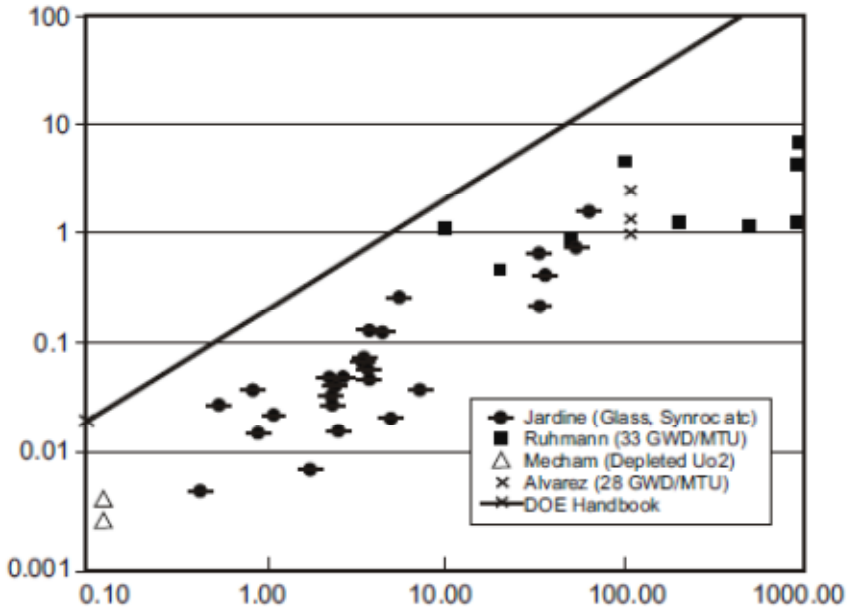

Figure 12 . Example Does Estimate for Oxidation and Collision (/Drop) of SNF Assemblies (after Kamas, et al., 2006) [copy right permission by ANS]

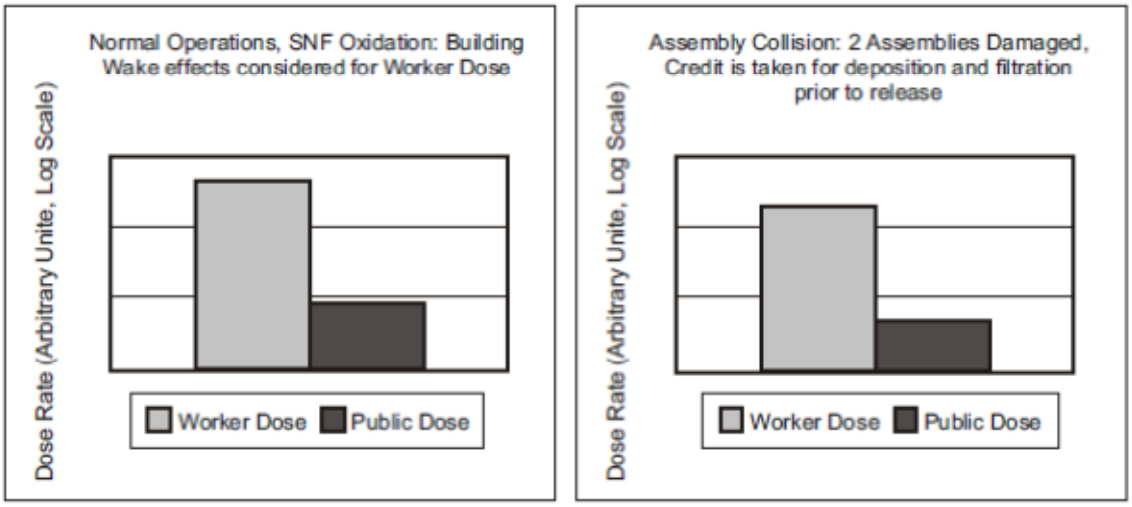

Figure 13. Hydride reorientation from circumferential (a) to radial (b) direction to hoop stress (Yagnik, et al., 2004); cladding thickness of ~0.6 mm [copy right permission by ANS]

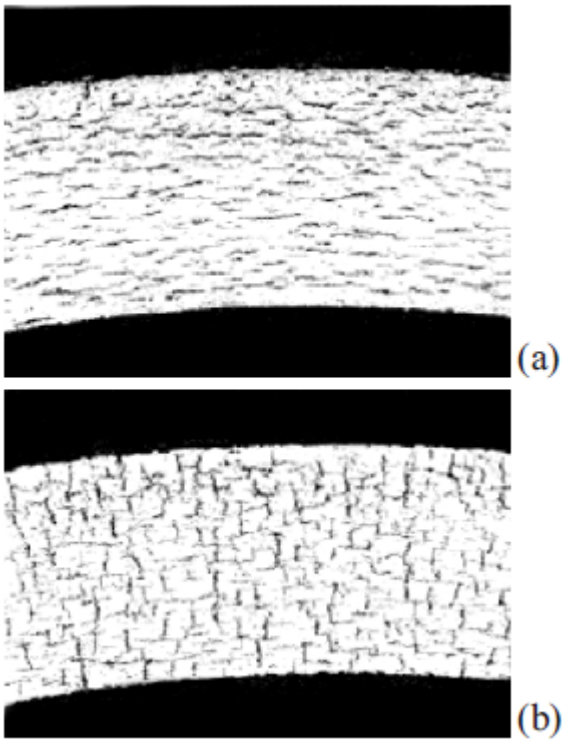

Figure 14. Effects of radial hydrides on ductility (elongation) loss in a more severe case. The different orientations result in different magnitudes of ductility loss (Yagnik, et al., 2004) [copy right permission by ANS]

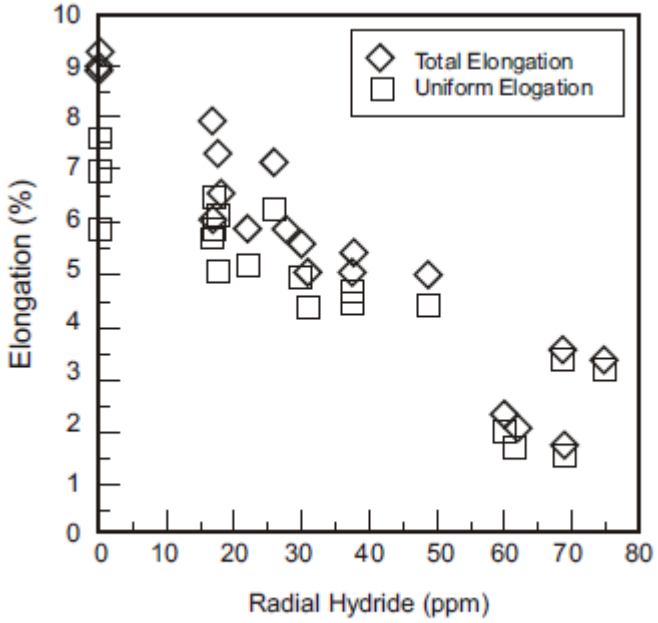

Figure 15. A schematic of Delayed-Hydride Cracking (DHC) process showing hydrogen diffusion to a existing crack tip. The threshold stress intensity factor for DHC of Zircaloy is in the range of 5 MPa $m^{1/2}$. Under storage conditions, such level of stress intensification has not been demonstrated, although a few possibilities are currently under study.

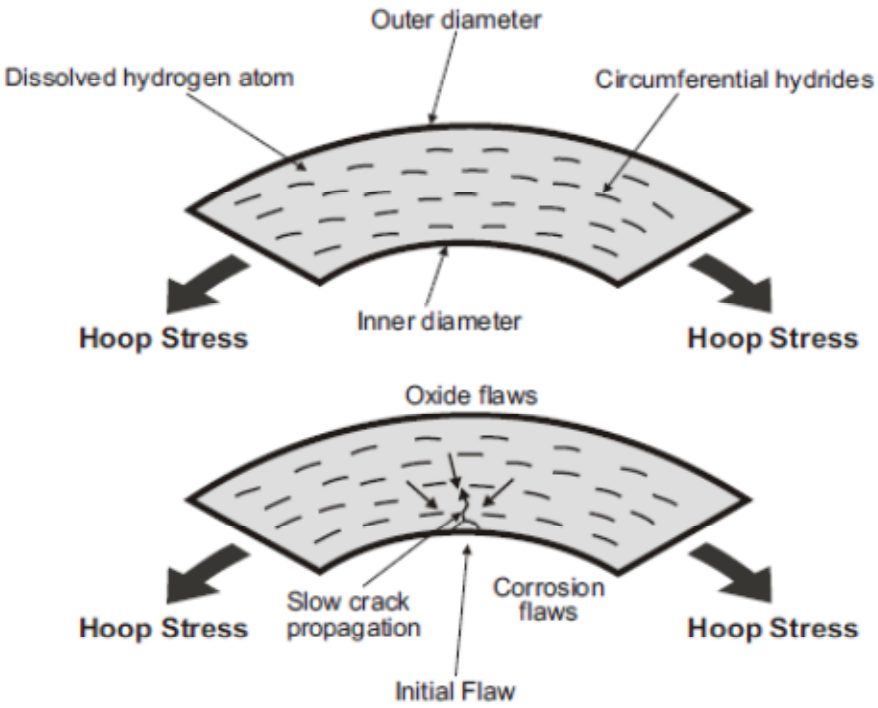

Figure 16. Cladding unzipping process by the oxidation/hydration of the SNF matrix or zirconium (DOE, 2002)

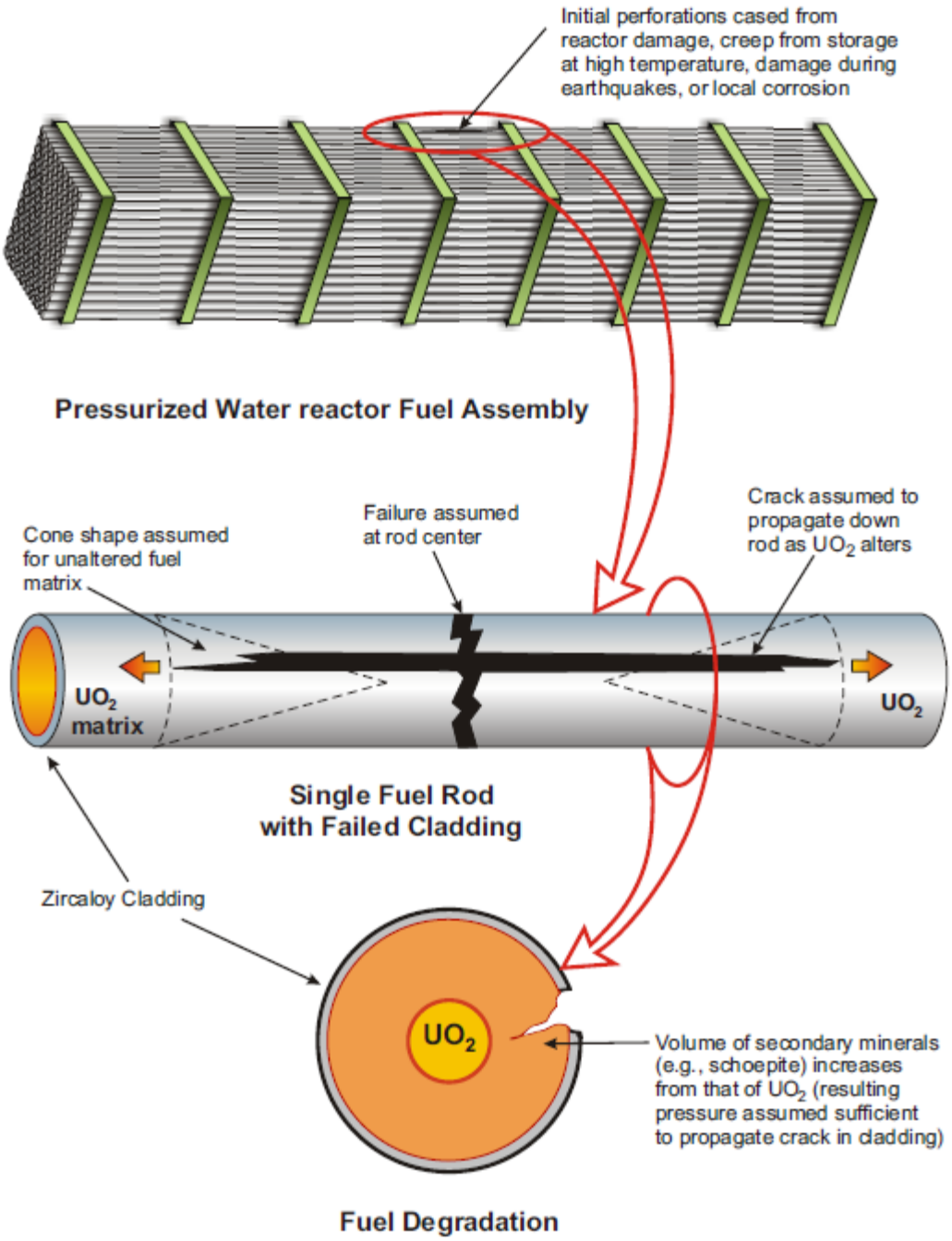

Table 1 Summary of SNF dissolution rates in oxidizing and reducing environments (Ahn, et al., 2011a). Spent (s) MOX fuel is also included in the table and the reference numbers quoted are from the reference by Ahn, et al. (2011a)

Parameter Name	Value	Description and Basis
Mobilization (Degradation) of Commercial SNF and sMOX (spent MOX) under the Oxidizing Condition (fraction per year; minimum and maximum)	3.00E-05, 6.00E-04 (log-uniform)	The oxidizing environment is considered because of the potential alpha radiolysis in the reducing environment and the early waste package failure. The assessment is more based on immersion conditions that are considered in the alternative disposal sites in the future.[9] The dissolution rate of Commercial SNF is assumed to bound that of sMOX under immersion conditions.[12] Both commercial SNF and sMOX have the particle size of ~ 1 mm after reactor irradiation. Other references include the references of [3] and [7].
Mobilization (Degradation) of Commercial SNF and sMOX under the Reducing Condition (fraction per year; minimum and maximum)	9.00E-07, 2.00E-05 (log-uniform)	An average factor of 0.03 (from 0.01 – 0.1) was factored in the oxidizing case. In the French and Belgian repositories, an average 2 x 10^{-6}/year was used [13], similar to the current estimate. To be consistent, the dissolution rate of sMOX was assumed to be same as the rate of commercial SNF [12].
Mobilization (Degradation) of Commercial SNF and sMOX under the Combined Condition (fraction per year; minimum and maximum)	9.00E-07, 6.00E-04 (log-uniform)	Because the alpha radiolysis may have limited effects on the dissolution rate of commercial SNF [14] and sMOX, the combined case is separated to represent some effects of alpha radiolysis. If we consider the hydrogen effects to be produced by the container corrosion, this combined rate could be conservative. The hydrogen could inhibit the SNF dissolution rate.[15] To be consistent, the dissolution rate of sMOX was assumed to be same as the rate of commercial SNF.[12]